

UC Irvine

UC Irvine Previously Published Works

Title

Characterizing the Dynamics of Proteasome Complexes by Proteomics Approaches

Permalink

<https://escholarship.org/uc/item/7gm7k0z5>

Journal

Antioxidants and Redox Signaling, 21(17)

ISSN

1523-0864

Authors

Kaake, Robyn M

Kao, Athit

Yu, Clinton

et al.

Publication Date

2014-12-10

DOI

10.1089/ars.2013.5815

Peer reviewed

FORUM REVIEW ARTICLE

Characterizing the Dynamics of Proteasome Complexes by Proteomics Approaches

Robyn M. Kaake, Athit Kao, Clinton Yu, and Lan Huang

Abstract

Significance: The proteasome is the degradation machine of the ubiquitin-proteasome system, which is critical in controlling many essential biological processes. Aberrant regulation of proteasome-dependent protein degradation can lead to various human diseases, and general proteasome inhibitors have shown efficacy for cancer treatments. Though clinically effective, current proteasome inhibitors have detrimental side effects and, thus, better therapeutic strategies targeting proteasomes are needed. Therefore, a comprehensive characterization of proteasome complexes will provide the molecular details that are essential for developing new and improved drugs. **Recent Advances:** New mass spectrometry (MS)-based proteomics approaches have been developed to study protein interaction networks and structural topologies of proteasome complexes. The results have helped define the dynamic proteomes of proteasome complexes, thus providing new insights into the mechanisms underlying proteasome function and regulation. **Critical Issues:** The proteasome exists as heterogeneous populations in tissues/cells, and its proteome is highly dynamic and complex. In addition, proteasome complexes are regulated by various mechanisms under different physiological conditions. Consequently, complete proteomic profiling of proteasome complexes remains a major challenge for the field. **Future Directions:** We expect that proteomic methodologies enabling full characterization of proteasome complexes will continue to evolve. Further advances in MS instrumentation and protein separation techniques will be needed to facilitate the detailed proteomic analysis of low-abundance components and subpopulations of proteasome complexes. The results will help us understand proteasome biology as well as provide new therapeutic targets for disease diagnostics and treatment. *Antioxid. Redox Signal.* 21, 2444–2456.

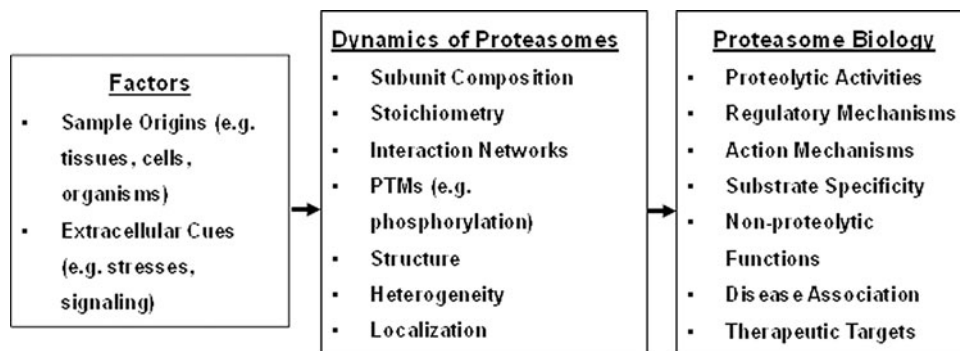
Introduction

PROTEOMES EXIST IN a state of constant flux—a dynamic equilibrium of protein synthesis and degradation in order to maintain cellular homeostasis. The ubiquitin-proteasome system (UPS) represents the major intracellular pathway for selective degradation of regulatory, misfolded, and damaged proteins in eukaryotic cells (24, 27, 36). Aberrant UPS regulation can result in irregular protein turnover and accumulation of dysfunctional proteins, thus leading to severe physiological repercussions and cytotoxicity. Not surprisingly, the disruption of normal UPS functions has been implicated in a broad range of human diseases, including various cancers and neurological disorders (28). Given their critical importance in cell biology, components of the

ubiquitin-proteasome degradation pathway have recently become attractive drug targets for the therapeutic intervention of a variety of human diseases (15, 28, 29). Therefore, a comprehensive characterization of the UPS is vital for our understanding of the molecular mechanisms underlying the pathologies of associated human diseases and for enabling us to design more effective treatment strategies targeting the UPS.

There are two major steps involved in the ubiquitin-dependent proteasome degradation pathway: (i) substrate polyubiquitination and (ii) substrate recognition and degradation by the proteasome. In the first step, a cascade of ubiquitination enzymes (E1, E2, and E3) mediates the conjugation of ubiquitin (Ub) chains to target proteins. A variety of ubiquitin chains have been identified, in which Ub is conjugated to one of seven internal

FIG. 1. Defining proteasome dynamics to understand proteasome biology. PTMs, posttranslational modifications.



lysine residues on the Ub molecule (24, 43, 83). Conventionally, K48-linked ubiquitin chains have been established as the major signal for targeted proteasomal degradation. However, recent studies have highlighted the importance of noncanonical linkages (K6, K11, K27, K29, K33, K63) in both proteasome- and nonproteasome-associated cellular processes (44–46, 83), notably with K11-linked ubiquitin chains being shown to be important in directing protein substrates for proteasome-dependent degradation. In the second step, a group of proteins called ubiquitin receptors have been suggested to recognize and transport ubiquitinated substrates to proteasomes for degradation (24).

The degradation machine of the UPS is the 26S proteasome, a ~2.5 MDa macromolecular protein complex composed of at least 33 subunits (24, 60). The 26S holocomplex contains two subcomplexes: the 20S catalytic core particle (CP) and the 19S regulatory particle (RP). The 20S CP is responsible for various proteolytic activities, and it has a highly conserved “barrel”-like structure consisting of two copies each of 14 nonidentical subunits (α 1–7, β 1–7) that are arranged into four heptameric rings stacked in the order of $\alpha_7\beta_7\beta_7\alpha_7$ (32, 54). While the 20S CP is capable of indiscriminately degrading peptides and small proteins in an ATP-independent manner, protein degradation carried out by the 26S proteasome complex is strictly ATP and ubiquitin dependent. In contrast to the 20S CP, the structures and functions of the 19S RP and 26S holocomplex are less well characterized. The latest innovative studies have revealed the topologies of the 19S RP and/or 26S holocomplex (8, 17, 42, 47, 48), thus providing new structural insights into molecular mechanisms underlying the diverse functions of the 19S RP, including substrate recognition and deubiquitination, protein unfolding, and translocation to the 20S CP for degradation.

Apart from the 19S RP, the 20S proteasome can be activated by three other known regulatory protein complexes, that is, PA28 α/β (also known as REG and the 11S regulator), PA28 γ /REGgamma, and PA200/Blm10, to form distinct functional subspecies of proteasomes (24, 60). In contrast to the 19S RP, these proteasome activator complexes do not have ATPase activity but can only assist ubiquitin-independent protein degradation with varied proteolytic cleavage specificities. PA28 α/β is mostly present in cytosol, which is IFN- γ inducible and responsible for generating MHC class I peptides for antigen presentation (68). In comparison, PA28 γ /REGgamma is localized in the nucleus, and it regulates the degradation of nuclear proteins such as steroid hormone receptor coactivator SRC-3 and cell cycle regulator p21 (52, 53).

Interestingly, PA200/Blm10 is also a nuclear proteasome regulator, and it has been suggested to play an important role in modulating normal spermatogenesis, DNA repair, and maintenance of mitochondria function (24, 64). In addition to multiple proteasome activators, the three 20S catalytic subunits (β 1, β 2, and β 5) can be replaced by three inducible subunits (β 1i, β 2i, and β 5i) in mammalian systems to form immunoproteasomes with altered proteolytic activities and functions. Recently, a novel and thymic-specific variant of β 5, that is, β 5t, has also been identified (57). Along with β 1i and β 2i, they can replace the three canonical catalytic β 1, β 2, and β 5 subunits and form thymoproteasomes that are critical for thymic education. Apart from subunit composition, proteasomes can be further modulated by posttranslational modifications (PTMs) and proteasome interacting proteins (PIPs) (1, 11, 16, 20, 24, 65, 79). It is evident that proteasome complexes in eukaryotic cells represent a dynamic and heterogeneous population, whose proteomes and functions can change depending on cell or tissue types, subcellular localization, and in response to extracellular cues (Fig. 1). One of the major goals in proteasome biology is to fully characterize proteasome subtypes with regard to their structures, compositions, PTMs, and associated proteins, and thus understand how the dynamics of proteasomal proteomes correlate with their diverse functionalities.

Despite its biological importance, our understanding of the regulation of the UPS and its associated components, especially proteasome complexes, remains elusive. Various technological advancements have made mass spectrometry (MS)-based proteomic approaches the primary method for characterizing and quantifying the dynamics of the proteomes of protein complexes (7). Such strategies have proved to be powerful and effective, and they have been successfully applied to unravel the molecular details of the UPS. For example, a series of proteomic studies have been carried out to map PTMs of proteasomes (55, 66), define the contents of ubiquitomes (43, 83), elucidate protein complex composition and structure, and decipher interaction landscapes of various protein complexes such as deubiquitinases, E3 ubiquitin ligases, and proteasomes (6, 8, 19, 31, 33, 38, 42, 48, 70, 77, 80, 81). The vast amount of information gained by proteomics studies has dramatically enhanced our current understanding of the UPS on a more systems level. The PTMs of proteasomes and their roles in regulating the proteasome function has been nicely reviewed recently by Cui *et al.* (16). Specific aspects on the phosphorylation and oxidation of proteasome complexes in cardiac tissues and their impact on

proteasome structures and activities are described by Drews (18) and Soriano *et al.* (69), respectively, in this Forum. Therefore, in this review, we focus on the recent developments in proteomics studies of proteasome complexes, particularly in the area of mapping protein interaction networks and protein complex structural topology. These studies represent a significant step forward toward a full understanding of the dynamic proteome of proteasome complexes and proteasomal biology.

Functional Characterization of Protein Interaction Networks of Proteasome Complexes by Quantitative Proteomics

Most proteins function in combination with other proteins *via* protein–protein interactions (PPIs). It is known that the disruption of endogenous PPIs, through environmental or genetic means, can have drastic effects on cell homeostasis. Many emerging therapeutic treatment strategies are now targeting protein interactions with new drugs being designed to disrupt harmful or disease causing PPIs (67, 82). Therefore, mapping the PPIs of macromolecular protein complexes is critical not only for a better understanding of health and disease, but also for predicting response to drug treatments and the design of future drug therapies.

Many studies have clearly shown that PPIs play a significant role in modulating proteasome functions (31, 35, 49, 65, 75, 77, 81). Given their dynamic nature, effective isolation of proteasome complexes from tissues and cells has been a major challenge in proteomic studies. Current approaches employed for isolating proteasome complexes for mass spectrometric analysis are summarized in Figure 2. There exists a delicate balance between isolating specific proteasome subtypes from heterogeneous populations and maintaining associated proteins, as many interactions are transient

and/or weak in nature. This tradeoff can impede comprehensive characterization of the proteasome interactome. Recent advances in protein purification strategies, especially the incorporation of chemical cross-linking, have provided researchers with the tools that are needed to expand our knowledge of proteasome interaction networks using MS-based quantitative proteomics (11, 39). Although various sample preparation strategies have been developed to facilitate the purification of proteasome complexes for MS characterization, each strategy has its own advantages and is beneficial for specific applications. For example, conventional biochemical approaches are best suited for isolating proteasomes from tissues and clinical samples, whereas affinity tag-based strategies are mostly attractive when cells can express tagged baits. While purifications under native conditions enable the isolation of functional proteasome entities for determining their subunit composition, stoichiometry, heterogeneity, PTMs and activities (31, 77–80), purifications under fully denaturing conditions permit better preservation of PTMs and can also be coupled with *in vivo* cross-linking to capture weak/transient protein interactions (33, 34, 39). Previous developments in proteasome purification strategies have been reviewed elsewhere (11, 20, 39, 79). In the next few sections, we review the recent advances made toward the mapping and functional characterization of various proteasome interaction networks, including those associated with cell cycle or stress response, as well as tissue- and cell-type specificities.

Mapping cell cycle-specific 26S proteasome interaction networks

Transitions between phases of the eukaryotic cell cycle are tightly controlled to maintain genome integrity and prevent uncontrolled cell proliferation. The UPS is key to the

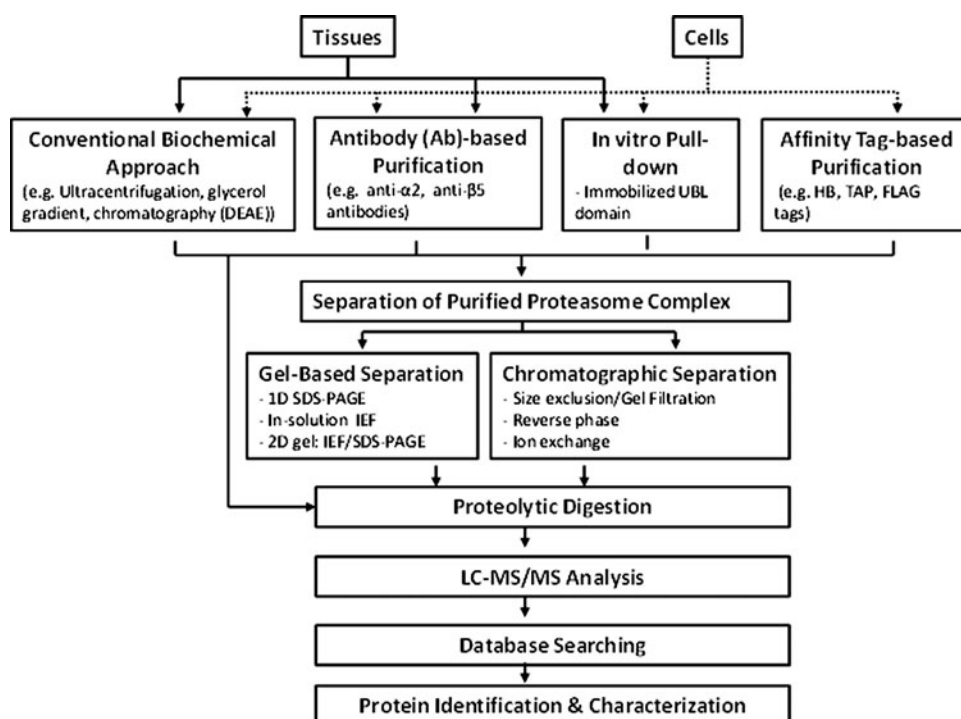


FIG. 2. The general workflow for isolating and analyzing proteasome complexes. DEAE, diethylaminoethyl; HB, histidine-biotin; IEF, isoelectric focusing; LC-MS/MS, liquid chromatography tandem mass spectrometry; SDS-PAGE, sodium dodecyl sulfate polyacrylamide gel electrophoresis; TAP, tandem affinity purification; UBL, ubiquitin-like.

regulation of cell cycle checkpoints and phase transitions (2, 5). By specifically and irreversibly degrading cyclins and other important cell cycle regulatory proteins, the UPS ensures the precise timing and unidirectional progression through the phases of the cell cycle. In order to better understand the molecular mechanisms underlying UPS regulation during the cell cycle, and specifically to identify novel regulators and targets of the 26S proteasome, our group developed and utilized the QTAX (quantitative analysis of tandem affinity purified *in vivo* cross-linked (x) protein complexes) method to purify 26S proteasome complexes from G1-, S-, and M-phase synchronized yeast cells, and then performed a comparative proteomic upon analysis on the resulting PPI networks (38). The schematic diagram of the QTAX method is displayed in Figure 3, which uniquely combines the following benefits: (i) stabilization of weak/transient interactions by *in vivo* chemical cross-linking; (ii) reduction of purification background by tandem affinity purification (TAP) under fully denaturing (*e.g.* 8 M urea) conditions *via* the HB tag (71); and (iii) unambiguous identification and quantitative characterization of specific PIPs by stable isotope labeling of amino acids in cell culture (SILAC)-based quantitative MS (33, 34, 38). The SILAC-based quantitation method enables us to distinguish specific PIPs from nonspecific background proteins based on their relative abundance ratios (*i.e.*, light/heavy or SILAC ratios) when comparing purified samples from cells expressing a tagged proteasome subunit and from untagged control cells (Fig. 3) (34). Essentially, if a protein is a background protein, it is purified in equal amounts from both the tagged and control cells, and all peptides representing that protein will be detected as a pair with an SILAC ratio of ~ 1 . In contrast, proteins that are enriched in the tagged sample and have a defined SILAC ratio (> 1.5) are considered putative PIPs (34). As for highly specific PIPs, they have the same SILAC profiles as proteasome subunits and are only found in tagged cells, not from control cells.

Using the QTAX method, we were able to capture, identify, and quantitatively compare 677 PIPs, 266 of which were not previously identified from unsynchronized cells, thus providing the largest detailed interaction map of the 26S proteasome to date (38). In comparison, 93% of the PIPs identified from unsynchronized cells in our previous reports (33, 34) were also present in our cell cycle study, confirming that QTAX-based experimental approaches are reproducible and robust. To identify trends within the data, each of the 677 PIPs was then classified into clusters based on their cell cycle-specific SILAC ratio profiles (38). As a result, 20 functionally significant groups of PIPs have been clustered, and 3 of them are enriched with cell cycle-related functions. Most excitingly, we have demonstrated for the first time that Fus3, an MAP kinase, physically interacts with the proteasome in a cell cycle phase-specific manner. Along with our results from studies on cell cycle-specific phosphorylation of proteasome subunits, we suspect that proteasomes may be regulated by Fus3-mediated phosphorylation through their direct physical interaction during pheromone-induced G1 arrest.

Stress-mediated dynamic changes in proteasome interaction networks

Oxidative stress has been implicated in aging as well as in a number of pathologies, including neurodegenerative dis-

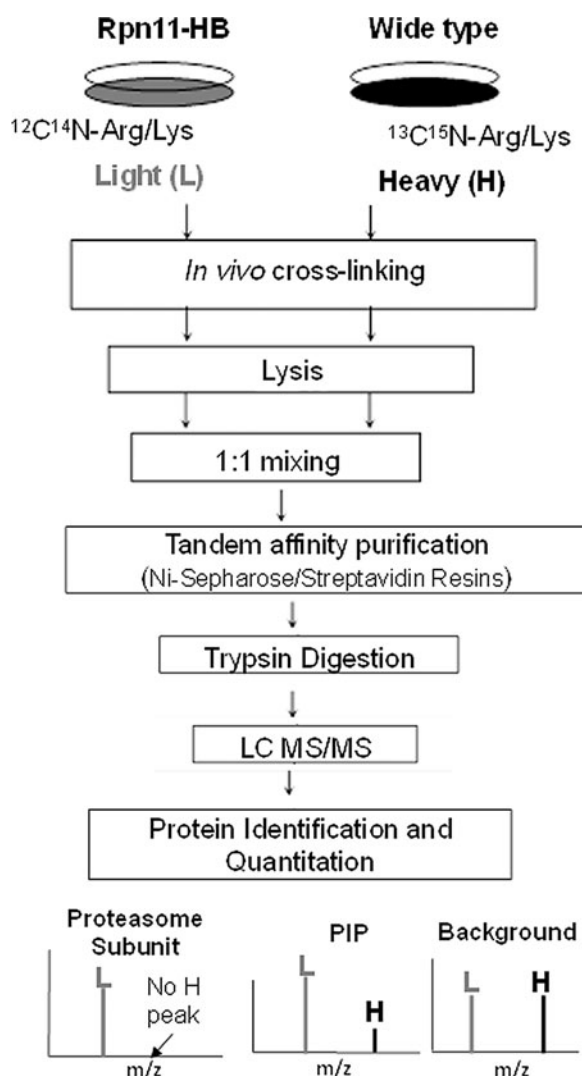


FIG. 3. Schematic diagram of the QTAX strategy. Cells expressing a His-Bio-tagged proteasome subunit (*i.e.*, Rpn11-HB) and a wild-type strain were grown in a light ($^{12}\text{C}^{14}\text{N}$ -Arg/Lys) and a heavy ($^{13}\text{C}^{15}\text{N}$ -Arg/Lys) containing media, respectively. After *in vivo* formaldehyde cross-linking, equal amounts of cell lysates were mixed for HB-tag based tandem affinity purification. The bound proteins were on-bead digested and analyzed by LC-MS/MS. Specific PIPs can be differentiated from background proteins with their SILAC ratios (L/H), based on the relative abundance ratios of Arg/Lys containing peptide pairs. Three groups of proteins were generally identified: (i) proteasome subunits; (ii) PIPs; and (iii) background proteins. PIPs, proteasome interacting proteins; QTAX, quantitative analysis of tandem affinity purified *in vivo* cross-linked (x) protein complexes.

orders and various cancers (13). Reactive oxygen species can cause oxidative damage to lipids, proteins, and DNA, and in the case of proteins, these modified molecules can either undergo chemical fragmentation or form large cytotoxic aggregates. Many studies have indicated the importance of the proteasome in the removal of oxidatively damaged proteins (1, 14). It appears that the 26S proteasome is more susceptible to oxidative stress, while the 20S proteasome is more resistant and plays a critical role in degrading oxidized

proteins. On acute H₂O₂-induced oxidative stress, the activity of the 26S proteasome is inhibited and 20S activity is enhanced (14, 81). Proteomic analysis of yeast 26S PIPs using affinity purification coupled with SILAC-based quantitative MS has revealed that oxidative stress triggers the dissociation of the 19S RP from the 20S CP, which is important for cell viability and cellular recovery from oxidative stress (81). Similarly, stress-induced disassembly of the 26S proteasome complex has also been demonstrated in mammalian cells, suggesting a general regulatory mechanism of the proteasome complex in response to oxidative stress (14, 61, 81). Interestingly, the dissociation of the 19S RP from the 20S CP in yeast is dependent on a known PIP, Ecm29, that is recruited to the 19S RP upon H₂O₂ stress (81). Recently, it has been shown that another PIP, heat shock protein 70 (Hsp70), appears to be responsible for mediating the dissociation and re-association of the 26S proteasome upon mild H₂O₂ treatment in mammalian cells (14). During cell recovery after H₂O₂ stress, regulatory proteins (PA28 $\alpha\beta$, PA28 γ , and PA200) were transcriptionally up-regulated, while 19S RP subunits remained unchanged (14, 61). Although the role for PA200 during oxidative stress response needs to be further addressed, studies have suggested that free 20S CP can be activated by poly(ADP ribose) polymerase and/or PA28 γ in the nucleus and by PA28 α/β in the cytoplasm to facilitate the ATP-independent degradation of oxidized proteins (14, 61). In addition, overexpression of PA28 α has been shown to enhance proteasome-mediated removal of misfolded and oxidized proteins, and to protect against H₂O₂-induced oxidative stress in cardiomyocytes (51). Taken together, these results have shown that the proteome of the proteasome complex changes dynamically in response to oxidative stress, which is associated with the recruitment of specific PIPs and/or reorganization of proteasome subpopulations. In addition, multiple regulatory mechanisms of the 26S and the 20S proteasomes exist and are important in cell survival, adaptation, and recovery in response to stress. However, whether Ecm29 and Hsp70 function similarly in yeast and mammalian cells and whether they work independently or in concert during oxidative stress require further investigation.

In addition to H₂O₂ stress, long-term alcohol treatment is cytotoxic and can lead to decreased proteasome activity and accumulation of ubiquitinated proteins (3, 12). To understand the effects of chronic ethanol feeding, changes in rat liver proteasome subunit composition and PIPs were investigated by analyzing endogenous proteasomes immunoprecipitated from ethanol-fed and control-fed rats. Several known PIPs were found to be differentially regulated with lower abundance in ethanol-fed proteasome samples: Ecm29, PA28 α , PA28 β , PA200, Usp14, and UCHL5/Uch37 (12). Decreased interactions between proteasome activators PA28 $\alpha\beta$ and PA200 with 20S proteasomes may lessen proteasomal ability to degrade oxidatively damaged proteins. In addition, abundance changes in the two different forms of proteasome subunit Adrm1 (native vs. cleaved forms) may affect ADRM1-mediated substrate translocation before their degradation. Though the molecular details underlying alcohol-induced regulation of the proteasome needs to be further explored, the results suggest that changes in proteomic profiles of proteasome complexes, including PIPs and composition, may contribute to the observed decrease in proteasome activities.

PIPs and subpopulations from various tissues/cell types

Recently, proteasome inhibitors have been presented as effective treatment strategies for cancer therapy (62). Bortezomib is the first general proteasome inhibitor approved for clinical use, and it has marked a new era for translational proteasome biology (29, 62). After its success, new proteasome inhibitors have been continuously developed to achieve better efficacy in cancer treatment. Though effective, treatment using general proteasome inhibitors has adverse and often dramatic side effects to other organs, which make long-term administration unfeasible. Therefore, in order to better understand and predict how different organs will react to proteasome inhibitors, various studies have set out to determine proteomic profiles of tissue-specific proteasomes.

In order to study endogenous proteasomes from tissues or cells, isolation of proteasomes is often carried out using conventional biochemical approaches (31, 86) and/or antibody-based immunoaffinity purification (Fig. 2) (10, 21, 22). Early proteomic characterization of murine heart proteasomes has identified their interactions with phosphatase PP2A and PKA (31, 86). It appears that PP2A and PKA have opposite effects on proteolytic activities, as the addition of PP2A inhibitor or recombinant active PKA *in vitro* led to increased proteolytic activity of cardiac proteasomes by modulating the phosphorylation of 20S proteasome subunits. Interestingly, a separate study by Zhang *et al.* has shown that PKA can phosphorylate 19S proteasome subunit Rpt6 (85), and this phosphorylation has a direct impact on proteasome activities, further suggesting that PKA is an important proteasomal regulator. In addition to PKA and PP2A, proteomic analysis of the murine cardiac and hepatic proteasomes has identified 7 additional PIPs, including elongation factor 2, 90 kDa heat shock protein, stress-70 protein mitochondrial precursor, calpain 2 catalytic subunit, NEDD8, CKII, and PP1(30). Except Nedd8 and PKA, orthologs of the other seven PIPs have also been identified in yeast proteasome interaction networks (33, 38), implying that these PIPs may have similar functional connections with proteasomes from both yeast and mammalian systems. Whether these PIPs contribute to observed differences in proteolytic activities between cardiac and hepatic proteasomes requires further investigation (30). Due to abundance differences in proteasomal regulatory proteins and inducible beta subunits, more complex mechanisms may be adopted for controlling functional diversity in proteasomes from different tissues.

In search of novel therapeutic targets in the myocardium (19), Drews *et al.* has undertaken a detailed proteomic analysis to dissect the functional and compositional diversity of subpopulations of 20S proteasomes in murine hearts. With the development of in-solution isoelectric focusing electrophoresis of multi-protein complexes that has an average resolution of 0.04 pH units, subpopulations of cardiac 20S proteasomes including constitutive proteasomes and immunoproteasomes, were isolated for functional characterization. The separated subgroups of proteasomes displayed different proteolytic activities, which correlate with compositional differences in their β subunits. In addition, cardiac and hepatic proteasomes appear to have similar subunit

compositions but different isoelectric points, and this is partially attributed to differences in proteasome phosphorylation states (19).

To further understand proteasome compositional heterogeneity, biochemical strategies have been used to isolate 20S proteasome complexes from mice heart, kidney, liver, lung, thymus, and spleen respectively (59). Subunit abundance was determined using a label-free quantitation method based on intensities of extracted ion chromatograms of peptides identified by LC-MS/MS. With this approach, it was determined that seven α subunits ($\alpha 1$ – $\alpha 7$) and five noncatalytic β subunits (*i.e.*, $\beta 3$, $\beta 4$, $\beta 6$, and $\beta 7$) have a similar abundance across the tissues analyzed, suggesting that the total amount of the 20S proteasome complex present in each tissue is similar. In comparison, the three constitutive catalytic subunits ($\beta 1$, $\beta 2$, and $\beta 5$), their inducible counterparts ($\beta 1i$, $\beta 2i$, and $\beta 5i$) and a thymus-specific subunit $\beta 5t$ have demonstrated preferential abundance in different tissues. As expected, $\beta 5t$ is most abundant in the thymus, and the three inducible β subunits appears to be elevated in the spleen and thymus that are more involved in immune response. In agreement with the study by Drews *et al.* (19), the relative abundance between the immunosubunits and their constitutive counterparts varies with tissues, suggesting the existence of tissue-variable hybrid classes of immunoproteasomes. These results add another layer of complexity that contributes to proteasome heterogeneity. In addition to 20S proteasomes, Wang *et al.* have recently investigated the dynamic proteomes of cardiac 19S proteasomes (77). With multi-dimensional chromatography-based purification strategy, two functionally distinct subpopulations of 19S regulatory complexes from murine hearts have been isolated and characterized (77). The major compositional difference between these two groups is heat shock protein 90 (Hsp90), which specifically attenuates the ability of one subgroup of the cardiac 19S proteasomes in regulating the 20S proteasome activities. Collectively, these studies have provided a strong molecular basis for designing specific agents against proteasome subpopulations for enhanced specificity in disease treatment.

Apart from tissues, human proteasomes have been isolated for proteomic analysis from human red blood cells using immunoprecipitation with a specific antibody against the 20S proteasome subunit $\alpha 2$ (MCP21 antibody) (10, 22). This antibody-based purification procedure can also be coupled with low% formaldehyde cross-linking to improve the capture of PIPs (10). In total, 86 proteins were identified, including all of the 26S proteasome subunits, the 20S inducible subunits, proteasome activators, inhibitors, and assembly proteins, as well as other proteins involved in the UPS (10). One of the novel putative PIPs Usp7, or herpes virus-associated ubiquitin-specific protease, was validated as a specific interactor of human 20S proteasomes; however, the functional consequence of this interaction is not clear. Compared with previous proteomic analyses of 26S proteasomes affinity purified from human HEK293 cells (78, 80), only 48 PIPs were found to overlap. This is most likely due to differences in affinity purification procedures, respective specific interactions with 20S and 26S proteasome, as well as cell types.

Recently, the same purification strategy has been coupled with a subcellular fractionation technique to study the proteomes of proteasome complexes in different subcellular

compartments (22). In combination with label-free quantitative MS, the subcellular distribution of the different proteasome subtypes was characterized (22). Quantitative comparison revealed a higher proportion of 19S regulator subunits as well as PA28 γ associated with nuclear 20S proteasomes, while a greater proportion of PA28 α/β was found in cytosolic fractions as expected (22). In addition, proteasome subunit Rpn11 and deubiquitinases Usp14 and UCHL5/Uch37 showed the highest association with nuclear 20S proteasomes, and the lowest association with cytosolic 20S proteasomes (22). In contrast, PI31, an inhibitor of proteasomes, was found to associate more with cytosolic proteasomes, and least with nuclear proteasomes. These results further support the notion that proteasomes exist as heterogeneous populations containing subcellular localization-dependent subproteomes in cells.

In addition to conventional biochemical and antibody-based immunoprecipitation methods, affinity purification strategies based on immobilized ubiquitin-like domains have been used as alternatives for isolating endogenous proteasomes from rat brains (72). In this work, proteasomes were isolated, and proteomes were compared from cytosolic and synaptosomal cellular fractions. LC-MS/MS analysis demonstrated that there was no detectable difference in the proteasome subunit composition for cytosolic and synaptosomal proteasomes (72). In addition to proteasome subunits, an additional 35 putative PIPs were captured and identified, including one cytosolic PIP (ECM29) and five synaptosomal PIPs (TAX1BP1, SNAP-25, drebin, GRASP-1, and 14-3-3 γ) (72). Expectedly, most of the shared PIPs were involved in UPS pathways and functions. Interestingly, when cultured hippocampal neurons were treated with glutamate receptor agonist NMDA (72), the disassembly of 26S proteasomes was also observed, which correlates well with a prolonged decrease in the activity of the UPS. Whether proteasome regulation during NMDA-induced synaptic plasticity is similar to that mediated by oxidative stress or combinatory regulatory mechanisms exist to counter different stresses remains to be explored. This study has shown that the proteomic profile of proteasomes can be altered by neuronal activity, and such interplay may affect synaptic plasticity and learning.

Structural Characterization of the 26S Proteasome Complex

Enormous efforts have been taken to uncover the structure of the 26S proteasome complex since its discovery; however, due to its heterogeneous and dynamic nature as well as the limitations in existing technologies; this task has proved extremely challenging. As an alternative, various attempts have been undertaken to define the structural details of the 20S CP and 19S RP subcomplexes, respectively. In the late 1990s, these efforts gave rise to the first crystal structure of the 20S CP from *Thermoplasma acidophilum*, which established itself as a 28-mer complex consisting of four heptameric rings assembled in a barrel-like shape (54). Unlike the 20S CP, which has a highly conserved and ordered structure, the 19S RP is less ordered, highly dynamic, and heterogeneous in nature and, thus, has proved to be much more difficult to characterize by traditional techniques such as X-ray crystallography and nuclear magnetic resonance. Therefore, alternative strategies based on low-resolution structural tools,

such as cryo-electron microscopy (cryoEM) and cross-linking mass spectrometry (XL-MS), have been developed and utilized to elucidate structures of the 19S RP and 26S holocomplex (4, 8, 9, 17, 26, 42, 47, 48, 58, 63, 73). These studies have provided new insights on the structural framework of the 26S proteasome, thus significantly improving our understanding of proteasome function (56). In this section, we review the latest technological advancements for the structural characterization of proteasome complexes.

Mapping the structural topology of proteasome complexes using XL-MS techniques

In addition to being powerful techniques for mapping PPI networks (23, 33, 34, 38), XL-MS strategies have the ability to define protein interaction interfaces through the identification of cross-linked peptides, and thus permit structural topology modeling of protein complexes (37, 40, 42, 48). Though XL-MS strategies have proved successful in the past, it has only been recently recognized as a robust alternative for protein structure analysis (50). This is largely due to innovative developments in cross-linking reagents, and substantial advancements in MS instrumentation and bioinformatics tools for data interpretation.

The unique combination of chemical cross-linking coupled with mass spectrometric and computational analysis for the elucidation of three-dimensional protein structures offers distinct advantages compared with traditional structural biology methods due to its speed, sensitivity, and versatility. Despite many advantages that XL-MS strategies possess, several challenges exist for this type of analysis, primarily due to the low abundance of cross-linked products and the inherent complexity of sequencing inter-linked peptides by MS (Fig. 4A). The complexity in peptide mixtures often impedes MS detection of low-abundance cross-linked

peptides due to the presence of significantly more abundant noncross-linked peptides. In addition, heterogeneous populations of cross-linked products, that is, inter-linked, intra-linked, and dead-end modified peptides, further complicate the analysis. This challenge can be overcome by a variety of methods with the use of enrichable and/or isotope-coded cross-linkers (50, 74). Apart from the detection of cross-linked peptides, unambiguous identification of inter-linked peptides by peptide sequencing is challenging when noncleavable cross-linkers are used. This is due to the difficulty in interpreting convoluted tandem mass spectra resulting from the fragmentation of two inter-linked peptides, though recent developments in new bioinformatics tools have made such data analysis possible with improved accuracy (76, 84). In order to circumvent these challenges and uncover the structural topologies of proteasome complexes, we have recently developed a novel integrated XL-MS strategy that facilitates MS detection and the identification of cross-linked products (41). This new strategy utilizes a novel homobifunctional amine-reactive, low-energy MS-cleavable cross-linker, disuccinimidyl sulfoxide (DSSO), and integrates chemical cross-linking with multistage tandem mass spectrometry (MS^n) and new bioinformatics tools. DSSO contains MS-cleavable sites that permit the preferential cleavage of the linker region in DSSO cross-linked peptides over the breakage of peptide bonds during collision-induced dissociation, thus enabling physical separation of a DSSO inter-linked peptide (α - β) into two single peptide chain fragment ions (α and β) during MS2 analysis (Fig. 4B). The resulting MS2 peptide fragment ions can be then subjected to peptide sequencing by MS3, which can be interpreted using existing database searching tools for easy peptide identification (41). The general workflow of the new DSSO based XL-MS strategy for elucidating structural topologies of proteasome complexes is illustrated in Figure 5. As shown, an integrative analysis of three types of MS^n data (MS1, MS2, and MS3) provides three lines of evidence to enable the identification of DSSO cross-linked peptides with a much higher confidence than using conventional noncleavable cross-linkers.

Our initial analysis of the 20S CP from *Saccharomyces cerevisiae* using the new DSSO based XL-MS strategy revealed 13 unique lysine-lysine linkages among the 20S CP subunits that were mapped onto its crystal structure within expected distances ($< 26 \text{ \AA}$) (41). The same strategy was also successfully applied to map subunit interaction interfaces of the 19S RP from *S. cerevisiae* (42). In total, 43 inter-subunit lysine-lysine inter-links were identified, representing 24 unique subunit-subunit binary interactions between the 19S subunits (42). In comparison to existing knowledge of protein subunit interactions, eight novel pair-wise interactions were determined for the first time in the yeast 19S RP (Table 1). In order to determine the architecture of the 19S RP, we developed a rigorous probabilistic analysis framework to generate a rationalized prediction of topological ordering of protein complexes that was solely based on experimentally derived cross-link data (42). The probabilistic analysis of identified lysine-lysine linkages within the ATPase base ring (Rpt1-6) of the 19S RP determined its topological ordering as Rpt1-2-6-3-4-5, which corroborated previous reports (8, 25, 58, 73). Although the architecture of the ATPase base ring was known at the time of our study, the topology of the

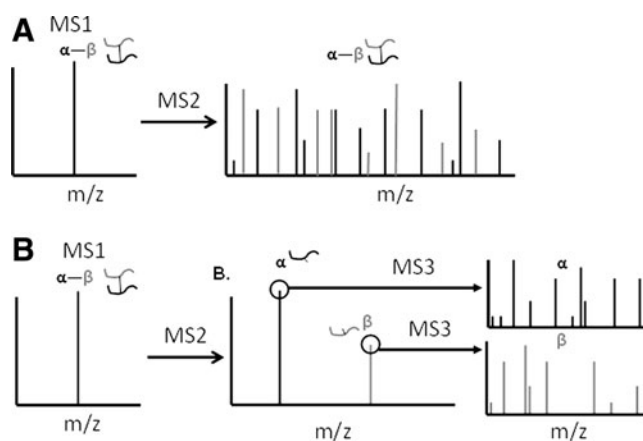


FIG. 4. MS sequencing of inter-linked peptides. (A) MS2 analysis of a noncleavable inter-linked peptide (α - β) results in a complex spectrum containing sequence ions from both peptides, which prevents it from being searched effectively by conventional database search engines; (B) MS2 analysis of an MS-cleavable inter-linked peptide detected in MS1, for example, a DSSO cross-linked peptide, results in the physical separation of α and β peptides, which enables their subsequent MS3 sequencing for unambiguous identification using conventional database search engines. DSSO, disuccinimidyl sulfoxide; MS, mass spectrometry.

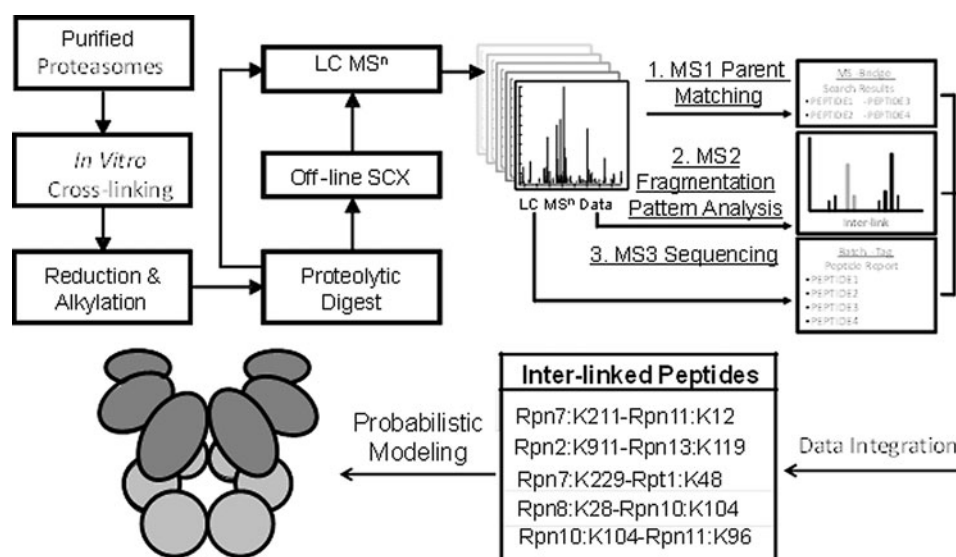


FIG. 5. The general workflow of DSSO-based XL-MS strategy for structure modeling of proteasome complexes. The purified proteasome complex was cross-linked *in vitro* with DSSO; the resulting products were digested, and subsequently separated and analyzed by LC MSⁿ. The resulting data provide three lines of evidence supporting the identification of DSSO cross-linked peptides: (i) Potential cross-linked peptides are determined based on the parent mass measured in MS1 through database searching using the MS-Bridge tool in Protein Prospector; (ii) characteristic fragmentation patterns from low-energy cleavage of DSSO cross-linked peptides results in a simple MS2 spectrum that contain peaks with specific mass relationships to their parent mass; and (iii) MS3 analysis of the individual peptide fragment ions detected in MS2 provides unambiguous peptide identification using conventional database searching methods such as Batch-Tag in Protein Prospector. Together, these three pieces of information are integrated and analyzed to enable the confident identification of cross-linked peptides. Cross-links that have been identified for the yeast 19S RP, representing binary inter-subunit interactions, are then used in a probabilistic modeling analysis to derive the spatial ordering of the 19S subcomplexes with the highest probability. MSⁿ, multistage tandem mass spectrometry; RP, regulatory particle; XL-MS, cross-linking mass spectrometry.

remainder of the 19S RP was not resolved. Therefore, we carried out a similar analysis to predict the spatial organization of the proteasome–CSN–eIF3 (PCI) domain-containing-heterohexamer, a part of the lid subcomplex of the 19S RP and composed of Rpn3, Rpn5, Rpn6, Rpn7, Rpn9, and Rpn12. The top scoring topology of the PCI-heterohexamer was determined as Rpn9-5-6-7-3-12 (42), in perfect agreement with recent results provided by other structural methods (47, 48). These results demonstrate the feasibility of combining the XL-MS strategy with probabilistic modeling to derive unknown spatial subunit organization of protein complexes.

Elucidating molecular architectures of the proteasome complexes using integrated approaches

Recently, two studies utilizing cryoEM based approaches elegantly defined the subunit architecture of the 19S RP and the 26S holocomplex (47, 48). Lander *et al.* (47) developed a new heterologous expression system, which was incorporated with cryoEM and single particle analysis to derive the topological structure of the yeast 19S RP and 26S proteasome. This integrated approach facilitated the localization of all subunits within the 19S RP and the delineation of their approximate subunit boundaries, thus providing a complete architectural picture of the proteasome. In comparison, Lasker *et al.* (48) employed a different and more comprehensive approach to probe the structure of the 26S holocomplex,

integrating data obtained from cryoEM, X-ray crystallography, and XL-MS, as well as previously known subunit interactions with comparative/homology modeling. This combinatory approach incorporated an XL-MS strategy involving a commercially available noncleavable cross-linker disuccinimidyl suberate (DSS) to determine protein interaction interfaces of purified *Schizosaccharomyces pombe* 26S proteasomes. In contrast to the DSSO-based XL-MS method (42), DSS cross-linked peptides result in complex MS2 spectra as shown in Figure 4A, which requires special database searching tools for data interpretation to eliminate false positives (76). The data obtained from all analyses were then translated into spatial restraints that enabled the fitting of atomic models into the density of the electron microscopy (EM) reconstruction (48), thus uncovering the molecular architecture of the 26S holocomplex.

These studies have determined that the lid subcomplex (consisting of Rpn3, Rpn5-9, Rpn11, and Rpn12) of the 19S RP is organized in a modular fashion with a horseshoe-shaped heterohexamer (Rpn3/5/6/7/9/12) and a heterodimer (Rpn8/Rpn11) (47, 48). Based on single-particle EM reconstructions of proteasome complexes, the 19S lid subcomplex was determined to localize on one side of the RP and to interact extensively with the base subcomplex, placing it also in close contact with the 20S CP. The PCI domain-containing-heterohexamer forms a horseshoe-shaped anchor structure, which possibly serves as a scaffold for the assembly of other 19S

TABLE 1. SUMMARY OF BINARY INTERSUBUNIT INTERACTIONS OF YEAST 26S PROTEASOME COMPLEX DETERMINED BY CROSS-LINKING MASS SPECTROMETRY AND OTHER BIOCHEMICAL METHODS

Subunits		Species	Method	Reference
Rpn1	Rpn10	sc	IVB	Other studies summarized in Ref. (48)
Rpn1	Rpt6	sc	IVB	Other studies summarized in Ref. (48)
Rpn2	Rpn3	sc	XL-MS	(48)
Rpn2	Rpn5	sc	XL-MS	(48)
Rpn2	Rpn9	sc	XL-MS	(48)
Rpn2	Rpn13	sc, sp	XL-MS, 2h	(42), other studies summarized in Ref. (48)
Rpn2	Rpt2	sc, sp	XL-MS	(42, 48)
Rpn2	Rpt6	sc, sp	XL-MS	(42)
Rpn3	Rpn5	sc	XL-MS	Other studies summarized in Ref. (48)
Rpn3	Rpn7	sc, sp	XL-MS	(42, 48)
Rpn3	Rpn8	sc	XL-MS	(42)
Rpn3	Rpn11	sc	IVB	Other studies summarized in Ref. (48)
Rpn3	Rpn12	sc	XL-MS, 2h	(42), other studies summarized in Ref. (48)
Rpn3	Rpn15	sc	XL-MS	(42), other studies summarized in Ref. (48)
Rpn5	Rpn6	sc	XL-MS, 2h	(42), other studies summarized in Ref. (48)
Rpn5	Rpn9	sc	XL-MS	(42, 48)
Rpn5	Rpt4	sc, sp	XL-MS	(48)
Rpn6	Rpn7	sc	XL-MS	(42)
Rpn6	Rpn11	sc	XL-MS	(42)
Rpn6	Rpt3	sc	XL-MS	(48)
Rpn6	Rpt4	sp	XL-MS	(48)
Rpn7	Rpn11	sc	XL-MS	(42)
Rpn7	Rpn15	sc	XL-MS	(42), other studies summarized in Ref. (48)
Rpn8	Rpn9	sc	XL-MS, 2h	(42), other studies summarized in Ref. (48)
Rpn8	Rpn10	sc	XL-MS	(42)
Rpn8	Rpn11	sc	XL-MS, 2h	(42), other studies summarized in Ref. (48)
Rpn9	Rpn11	sc	2h	Other studies summarized in Ref. (48)
Rpn9	Rpt5	sc	XL-MS	(42)
Rpn10	Rpn11	sc	XL-MS	(42)
Rpn10	Rpt5	sp	XL-MS	(48)
Rpn11	Rpn3	sp	XL-MS	(48)
Rpn11	Rpt3	sp	XL-MS	(48)
Rpn11	Rpt6	sc	XL-MS	(48)
Rpt1	Rpt2	sc, sp	XL-MS	(42, 48)
Rpt1	Rpt3	sp	XL-MS	(48)
Rpt1	Rpt4	sp	XL-MS	(48)
Rpt1	Rpt5	sc	XL-MS	(42, 48)
Rpt1	Rpt6	sc	XL-MS	(42)
Rpt1	$\alpha 4$	sc, sp	XL-MS	(48)
Rpt1	$\alpha 5$	sc	XL-MS	(48)
Rpt2	Rpt6	sc, sp	XL-MS	(42, 48)
Rpt3	Rpt4	sc, sp	XL-MS	(48)
Rpt3	Rpt5	sp	XL-MS, 2h	(48)
Rpt3	Rpt6	sc, sp	XL-MS	(42, 48)
Rpt4	Rpt5	sc, sp	XL-MS	(42, 48)
Rpt4	Rpt6	sc	2h	Other studies summarized in Ref. (48)
Rpt4	$\alpha 1$	sp	XL-MS	(48)
Rpt4	$\alpha 4$	sc	2h	Other studies summarized in Ref. (48)
Rpt6	$\alpha 2$	sp	XL-MS	(48)
$\alpha 1$	$\alpha 2$	sc, sp	XL-MS	(48)
$\alpha 1$	$\alpha 7$	sp	XL-MS	(48)
$\alpha 2$	$\alpha 3$	sp	XL-MS	(48)
$\alpha 3$	$\beta 3$	sc	XL-MS	(41)
$\alpha 6$	$\alpha 7$	sp	XL-MS	(48)
$\alpha 6$	$\beta 6$	sc	XL-MS	(41)
$\beta 3$	$\beta 4$	sc	XL-MS	(41)

sc, *Saccharomyces cerevisiae*; sp, *Schizosaccharomyces pombe*; 2h, yeast 2-hybrid system; IVB, *in vitro* binding assay; XL-MS, cross-linking mass spectrometry.

subunits, as they are determined as the hinge between the base and the rest of the lid (47, 48). Rpn11, the only essential deubiquitinase of the proteasome, is located at the mouth of the horse-shoe structure and interacts extensively with Rpn8, Rpn9, and Rpn5. Rpn2 contacts the Rpn8/11 dimer at its torus-shaped region, and it interacts with Rpn12 and Rpn3 at its distal end (48). In addition, Rpn2 associates with Rpt2 and Rpt6, and its C-terminus physically interacts with Rpn13 (42, 48). In comparison, Rpn1 is conformationally variable and positioned at the periphery of the ATPase ring (48). Moreover, the two ubiquitin receptors (Rpn10 and Rpn13) and a deubiquitinase (Rpn11) appear to be in a forked arrangement with Rpn11 in the center bottom and the two receptors in the top corners (9, 48). This suggests an arrangement where the polyUb chain of a protein substrate is bound to the distal receptors, and the base of the chain is exposed to the deubiquitinase. Furthermore, the extensive and unexpected contacts between the 19S lid and 20S CP may be important in stabilizing the entire holocomplex assembly, and/or be a part of an allosteric network that modulates the activities of either subcomplex (47, 48). Taken together, these studies have not only determined the subunit organization of the 19S RP structure, but also defined the entire architecture of the 26S proteasome for the first time (47, 48). The structural details obtained offer novel insights into the mechanisms of ubiquitin binding, deubiquitination, substrate unfolding, and translocation by the proteasome.

In comparison to these reports, it is noted that our DSSO XL-MS strategy was able to determine two additional interactions between the small Rpn15/Sem1 subunit to Rpn3 and Rpn7 respectively, which were not detected by other approaches (47, 48). This finding was later confirmed by a more targeted approach through EM difference mapping between wild-type Rpn15 and an Rpn15 deletion strain (9). This further indicates that XL-MS analysis can provide complementary information to EM-based structural analysis, and combinatory approaches integrating various technologies are beneficial in the structural characterization of heterogeneous and dynamic protein complexes such as proteasomes.

Summary

MS-based proteomic studies have revealed that the dynamic proteome of proteasome complexes is much more complicated than anticipated. Given the importance that PIPs play in modulating proteasome assembly, PTMs, activity, and function, more detailed proteomic studies mapping the reorganization of proteasome interaction networks, induced by various cytotoxic stresses from different cell types, tissues, and organisms, are clearly needed and essential to address many unanswered questions in our understanding of proteasome regulation. In addition, the profiling of dynamic proteomes of proteasome complexes at different disease states will help unravel the molecular mechanisms underlying human pathologies.

Significant progress has been made while defining the structural topologies of the 19S RP and the 26S holocomplex, which is largely attributed to the innovative development of novel low-resolution structural methods. The integration of improved technologies, including cryoEM, XL-MS, and computational modeling, has allowed the characterization of

the architectures of proteasome complexes possible, and has made major contributions to our current structural understanding of the 26S proteasome. The work presented here represents a huge step forward toward the full understanding of the heterogeneous and dynamic proteasome complex. We expect that technological advancements in structural and proteomic methods will be further developed to enable a full characterization of proteasome complexes, and, thus, increase our understanding of proteasomal biology as well as provide new therapeutic targets for disease diagnostics and treatment.

Acknowledgments

This work is supported by NIH R21CA161807 and R01GM074830 to L.H., and by R01GM106003 to L.H. and S.R.

References

1. Aiken CT, Kaake RM, Wang X, and Huang L. Oxidative stress-mediated regulation of proteasome complexes. *Mol Cell Proteomics* 10: R110.006924, 2011.
2. Ang XL and Wade Harper J. SCF-mediated protein degradation and cell cycle control. *Oncogene* 24: 2860–2870, 2005.
3. Bardag-Gorce F. Effects of ethanol on the proteasome interacting proteins. *World J Gastroenterol* 16: 1349–1357, 2010.
4. Beck F, Unverdorben P, Bohn S, Schweitzer A, Pfeifer G, Sakata E, Nickell S, Plitzko JM, Villa E, Baumeister W, and Forster F. Near-atomic resolution structural model of the yeast 26S proteasome. *Proc Natl Acad Sci U S A* 109: 14870–14875, 2012.
5. Benanti JA. Coordination of cell growth and division by the ubiquitin-proteasome system. *Semin Cell Dev Biol* 23: 492–498, 2012.
6. Bennett EJ, Rush J, Gygi SP, and Harper JW. Dynamics of cullin-RING ubiquitin ligase network revealed by systematic quantitative proteomics. *Cell* 143: 951–965, 2010.
7. Bensimon A, Heck AJ, and Aebersold R. Mass spectrometry-based proteomics and network biology. *Annu Rev Biochem* 81: 379–405, 2012.
8. Bohn S, Beck F, Sakata E, Walzthoeni T, Beck M, Aebersold R, Forster F, Baumeister W, and Nickell S. Structure of the 26S proteasome from *Schizosaccharomyces pombe* at subnanometer resolution. *Proc Natl Acad Sci U S A* 107: 20992–20997, 2010.
9. Bohn S, Sakata E, Beck F, Pathare GR, Schnitger J, Nagy I, Baumeister W, and Förster F. Localization of the regulatory particle subunit Sem1 in the 26S proteasome. *Biochem Biophys Res Commun* 435: 250–254, 2013.
10. Bousquet-Dubouch MP, Baudalet E, Guerin F, Matondo M, Uttenweiler-Joseph S, Burlet-Schiltz O, and Monsarrat B. Affinity purification strategy to capture human endogenous proteasome complexes diversity and to identify proteasome-interacting proteins. *Mol Cell Proteomics* 8: 1150–1164, 2009.
11. Bousquet-Dubouch MP, Fabre B, Monsarrat B, and Burlet-Schiltz O. Proteomics to study the diversity and dynamics of proteasome complexes: from fundamentals to the clinic. *Expert Rev Proteomics* 8: 459–481, 2011.
12. Bousquet-Dubouch MP, Nguen S, Bouyssié D, Burlet-Schiltz O, French SW, Monsarrat B, and Bardag-Gorce F. Chronic ethanol feeding affects proteasome-interacting proteins. *Proteomics* 9: 3609–3622, 2009.

13. Breusing N and Grune T. Regulation of proteasome-mediated protein degradation during oxidative stress and aging. *Biol Chem* 389: 203–209, 2008.
14. Chondrogianni N, Petropoulos I, Grimm S, Georgila K, Catalgol B, Friguet B, Grune T, and Gonos ES. Protein damage, repair and proteolysis. *Mol Aspects Med* 35: 1–71, 2014.
15. Ciechanover A. Intracellular protein degradation: from a vague idea thru the lysosome and the ubiquitin-proteasome system and onto human diseases and drug targeting. *Biochim Biophys Acta* 1824: 3–13, 2012.
16. Cui Z, Scruggs SB, Gilda JE, Ping P, and Gomes AV. Regulation of cardiac proteasomes by ubiquitination, SUMOylation, and beyond. *J Mol Cell Cardiol* pii: S0022-2828(13)00307-6, 2013.
17. da Fonseca PC, He J, and Morris EP. Molecular model of the human 26S proteasome. *Mol Cell* 46: 54–66, 2012.
18. Drews O. The left and right ventricles in the grip of protein degradation: Similarities and unique patterns in regulation. *J Mol Cell Cardiol* 2014 [Epub ahead of print]; doi:10.1016/j.yjmcc.2014.02.016.
19. Drews O, Wildgruber R, Zong C, Sukop U, Nissum M, Weber G, Gomes AV, and Ping P. Mammalian proteasome subpopulations with distinct molecular compositions and proteolytic activities. *Mol Cell Proteomics* 6: 2021–2031, 2007.
20. Drews O, Zong C, and Ping P. Exploring proteasome complexes by proteomic approaches. *Proteomics* 7: 1047–1058, 2007.
21. Ducoux-Petit M, Uttenweiler-Joseph S, Brichory F, Bousquet-Dubouch MP, Burlet-Schiltz O, Haeuw JF, and Monsarrat B. Scaled-down purification protocol to access proteomic analysis of 20S proteasome from human tissue samples: comparison of normal and tumor colorectal cells. *J Proteome Res* 7: 2852–2859, 2008.
22. Fabre B, Lambour T, Delobel J, Amalric F, Monsarrat B, Burlet-Schiltz O, and Bousquet-Dubouch MP. Subcellular distribution and dynamics of active proteasome complexes unraveled by a workflow combining *in vivo* complex cross-linking and quantitative proteomics. *Mol Cell Proteomics* 12: 687–699, 2013.
23. Fang L, Kaake RM, Patel VR, Yang Y, Baldi P, and Huang L. Mapping the protein interaction network of the human COP9 signalosome complex using a label-free QTAX Strategy. *Mol Cell Proteomics* 11: 138–147, 2012.
24. Finley D. Recognition and processing of ubiquitin-protein conjugates by the proteasome. *Annu Rev Biochem* 78: 477–513, 2009.
25. Forster F, Lasker K, Beck F, Nickell S, Sali A, and Baumeister W. An atomic model AAA-ATPase/20S core particle sub-complex of the 26S proteasome. *Biochem Biophys Res Commun* 388: 228–233, 2009.
26. Forster F, Lasker K, Nickell S, Sali A, and Baumeister W. Toward an integrated structural model of the 26S proteasome. *Mol Cell Proteomics* 9: 1666–1677, 2010.
27. Goldberg AL. Protein degradation and protection against misfolded or damaged proteins. *Nature* 426: 895–899, 2003.
28. Goldberg AL. Functions of the proteasome: from protein degradation and immune surveillance to cancer therapy. *Biochem Soc Trans* 35: 12–17, 2007.
29. Goldberg AL. Development of proteasome inhibitors as research tools and cancer drugs. *J Cell Biol* 199: 583–588, 2012.
30. Gomes AV, Young GW, Wang Y, Zong C, Eghbali M, Drews O, Lu H, Stefani E, and Ping P. Contrasting proteome biology and functional heterogeneity of the 20 S proteasome complexes in mammalian tissues. *Mol Cell Proteomics* 8: 302–315, 2009.
31. Gomes AV, Zong C, Edmondson RD, Li X, Stefani E, Zhang J, Jones RC, Thyparambil S, Wang GW, Qiao X, Bardag-Gorce F, and Ping P. Mapping the murine cardiac 26S proteasome complexes. *Circ Res* 99: 362–371, 2006.
32. Groll M, Ditzel L, Löwe J, Stock D, Bochtler M, Bartunik HD, and Huber R. Structure of 20S proteasome from yeast at 2.4 Å resolution. *Nature* 386: 463–471, 1997.
33. Guerrero C, Milenkovic T, Przulj N, Kaiser P, and Huang L. Characterization of the proteasome interaction network using a QTAX-based tag-team strategy and protein interaction network analysis. *Proc Natl Acad Sci U S A* 105: 13333–13338, 2008.
34. Guerrero C, Tagwerker C, Kaiser P, and Huang L. An integrated mass spectrometry-based proteomic approach: quantitative analysis of tandem affinity-purified *in vivo* cross-linked protein complexes (QTAX) to decipher the 26 S proteasome-interacting network. *Mol Cell Proteomics* 5: 366–378, 2006.
35. Guo X, Engel JL, Xiao J, Tagliabracci VS, Wang X, Huang L, and Dixon JE. UBLCP1 is a 26S proteasome phosphatase that regulates nuclear proteasome activity. *Proc Natl Acad Sci U S A* 108: 18649–18654, 2011.
36. Hershko A and Ciechanover A. The ubiquitin system. *Annu Rev Biochem* 67: 425–479, 1998.
37. Herzog F, Kahraman A, Boehringer D, Mak R, Bracher A, Walzthoeni T, Leitner A, Beck M, Hartl FU, Ban N, Malmstrom L, and Aebersold R. Structural probing of a protein phosphatase 2A network by chemical cross-linking and mass spectrometry. *Science* 337: 1348–1352, 2012.
38. Kaake RM, Milenkovic T, Przulj N, Kaiser P, and Huang L. Characterization of cell cycle specific protein interaction networks of the yeast 26S proteasome complex by the QTAX strategy. *J Proteome Res* 9: 2016–2029, 2010.
39. Kaake RM, Wang X, and Huang L. Profiling of protein interaction networks of protein complexes Using affinity purification and quantitative mass spectrometry. *Mol Cell Proteomics* 9: 1650–1665, 2010.
40. Kalisman N, Adams CM, and Levitt M. Subunit order of eukaryotic TriC/CCT chaperonin by cross-linking, mass spectrometry, and combinatorial homology modeling. *Proc Natl Acad Sci U S A* 109: 2884–2889, 2012.
41. Kao A, Chiu C, Vellucci D, Yang Y, Patel V, Guan S, Randall A, Baldi P, Rychnovsky S, and Huang L. Development of a novel cross-linking strategy for fast and accurate identification of cross-linked peptides of protein complexes. *Mol Cell Proteomics* 10: M110.002212, 2011.
42. Kao A, Randall A, Yang Y, Patel VR, Kandur W, Guan S, Rychnovsky SD, Baldi P, and Huang L. Mapping the structural topology of the yeast 19S proteasomal regulatory particle using chemical cross-linking and probabilistic modeling. *Mol Cell Proteomics* 11: 1566–1577, 2012.
43. Kim W, Bennett EJ, Huttlin EL, Guo A, Li J, Possemato A, Sowa ME, Rad R, Rush J, Comb MJ, Harper JW, and Gygi SP. Systematic and quantitative assessment of the ubiquitin-modified proteome. *Mol Cell* 44: 325–340, 2011.
44. Kravtsova-Ivantsiv Y and Ciechanover A. Non-canonical ubiquitin-based signals for proteasomal degradation. *J Cell Sci* 125: 539–548, 2012.

45. Kravtsova-Ivantsiv Y, Sommer T, and Ciechanover A. The lysine48-based polyubiquitin chain proteasomal signal: not a single child anymore. *Angew Chem Int Ed Engl* 52: 192–198, 2013.
46. Kulathu Y and Komander D. Atypical ubiquitylation—the unexplored world of polyubiquitin beyond Lys48 and Lys63 linkages. *Nat Rev Mol Cell Biol* 13: 508–523, 2012.
47. Lander GC, Estrin E, Matyskiela ME, Bashore C, Nogales E, and Martin A. Complete subunit architecture of the proteasome regulatory particle. *Nature* 482: 186–191, 2012.
48. Lasker K, Forster F, Bohn S, Walzthoeni T, Villa E, Unverdorben P, Beck F, Aebersold R, Sali A, and Baumeister W. Molecular architecture of the 26S proteasome holo-complex determined by an integrative approach. *Proc Natl Acad Sci U S A* 109: 1380–1387, 2012.
49. Leggett DS, Hanna J, Borodovsky A, Crosas B, Schmidt M, Baker RT, Walz T, Ploegh H, and Finley D. Multiple associated proteins regulate proteasome structure and function. *Mol Cell* 10: 495–507, 2002.
50. Leitner A, Walzthoeni T, Kahraman A, Herzog F, Rinner O, Beck M, and Aebersold R. Probing native protein structures by chemical cross-linking, mass spectrometry and bioinformatics. *Mol Cell Proteomics* 9: 1634–1649, 2010.
51. Li J, Powell SR, and Wang X. Enhancement of proteasome function by PA28 α overexpression protects against oxidative stress. *FASEB J* 25: 883–893, 2011.
52. Li X, Amazit L, Long W, Lonard DM, Monaco JJ, and O'Malley BW. Ubiquitin- and ATP-independent proteolytic turnover of p21 by the REG γ -proteasome pathway. *Mol Cell* 26: 831–842, 2007.
53. Li X, Lonard DM, Jung SY, Malovannaya A, Feng Q, Qin J, Tsai SY, Tsai MJ, and O'Malley BW. The SRC-3/AIB1 coactivator is degraded in a ubiquitin- and ATP-independent manner by the REG γ proteasome. *Cell* 124: 381–392, 2006.
54. Löwe J, Stock D, Jap B, Zwickl P, Baumeister W, and Huber R. Crystal structure of the 20S proteasome from the archaeon *T. acidophilum* at 3.4 Å resolution. *Science* 268: 533–539, 1995.
55. Lu H, Zong C, Wang Y, Young GW, Deng N, Souda P, Li X, Whitelegge J, Drews O, Yang PY, and Ping P. Revealing the dynamics of the 20 S proteasome phosphoproteome: a combined CID and electron transfer dissociation approach. *Mol Cell Proteomics* 7: 2073–2089, 2008.
56. Matyskiela ME, Lander GC, and Martin A. Conformational switching of the 26S proteasome enables substrate degradation. *Nat Struct Mol Biol* 20: 781–788, 2013.
57. Murata S, Sasaki K, Kishimoto T, Niwa S, Hayashi H, Takahama Y, and Tanaka K. Regulation of CD8⁺ T cell development by thymus-specific proteasomes. *Science* 316: 1349–1353, 2007.
58. Nickell S, Beck F, Scheres SH, Korinek A, Forster F, Lasker K, Mihalache O, Sun N, Nagy I, Sali A, Plitzko JM, Carazo JM, Mann M, and Baumeister W. Insights into the molecular architecture of the 26S proteasome. *Proc Natl Acad Sci U S A* 106: 11943–11947, 2009.
59. Pelletier S, Schuurman KG, Berkers CR, Ovaa H, Heck AJ, and Raijmakers R. Quantifying cross-tissue diversity in proteasome complexes by mass spectrometry. *Mol Biosyst* 6: 1450–1453, 2010.
60. Pickart CM and Cohen RE. Proteasomes and their kin: proteases in the machine age. *Nat Rev Mol Cell Biol* 5: 177–187, 2004.
61. Pickering AM and Davies KJ. Differential roles of proteasome and immunoproteasome regulators Pa28 α , Pa28 γ and Pa200 in the degradation of oxidized proteins. *Arch Biochem Biophys* 523: 181–190, 2012.
62. Rastogi N and Mishra DP. Therapeutic targeting of cancer cell cycle using proteasome inhibitors. *Cell Div* 7: 26, 2012.
63. Sakata E, Bohn S, Mihalache O, Kiss P, Beck F, Nagy I, Nickell S, Tanaka K, Saeki Y, Forster F, and Baumeister W. Localization of the proteasomal ubiquitin receptors Rpn10 and Rpn13 by electron cryomicroscopy. *Proc Natl Acad Sci U S A* 109: 1479–1484, 2012.
64. Savulescu AF and Glickman MH. Proteasome activator 200: the heat is on. *Mol Cell Proteomics* 10: R110.006890, 2011.
65. Schmidt M, Hanna J, Elsasser S, and Finley D. Proteasome-associated proteins: regulation of a proteolytic machine. *Biol Chem* 386: 725–737, 2005.
66. Scruggs SB, Zong NC, Wang D, Stefani E, and Ping P. Post-translational modification of cardiac proteasomes: functional delineation enabled by proteomics. *Am J Physiol Heart Circ Physiol* 303: H9–H18, 2012.
67. Shangary S and Wang S. Small-molecule inhibitors of the MDM2-p53 protein-protein interaction to reactivate p53 function: a novel approach for cancer therapy. *Annu Rev Pharmacol Toxicol* 49: 223–241, 2009.
68. Sijts EJ and Kloetzel PM. The role of the proteasome in the generation of MHC class I ligands and immune responses. *Cell Mol Life Sci* 68: 1491–1502, 2011.
69. Soriano GP, De Bruin G, Overkleeft HS, and Florea BI. Toward understanding induction of oxidative stress and apoptosis by proteasome inhibitors. *Antioxid Redox Signal* 21: 2419–2443, 2014.
70. Sowa ME, Bennett EJ, Gygi SP, and Harper JW. Defining the human deubiquitinating enzyme interaction landscape. *Cell* 138: 389–403, 2009.
71. Tagwerker C, Flick K, Cui M, Guerrero C, Dou Y, Auer B, Baldi P, Huang L, and Kaiser P. A tandem affinity tag for two-step purification under fully denaturing conditions: application in ubiquitin profiling and protein complex identification combined with in vivo cross-linking. *Mol Cell Proteomics* 5: 737–748, 2006.
72. Tai HC, Besche H, Goldberg AL, and Schuman EM. Characterization of the brain 26S proteasome and its interacting proteins. *Front Mol Neurosci* 3: pii:12, 2010.
73. Tomko RJ, Jr., Funakoshi M, Schneider K, Wang J, and Hochstrasser M. Heterohexameric ring arrangement of the eukaryotic proteasomal ATPases: implications for proteasome structure and assembly. *Mol Cell* 38: 393–403, 2010.
74. Vellucci D, Kao A, Kaake RM, Rychnovsky SD, and Huang L. Selective enrichment and identification of azide-tagged cross-linked peptides using chemical ligation and mass spectrometry. *J Am Soc Mass Spectrom* 21: 1432–1445, 2010.
75. Verma R, Chen S, Feldman R, Schieltz D, Yates J, Dohmen J, and Deshaies RJ. Proteasomal proteomics: identification of nucleotide-sensitive proteasome-interacting proteins by mass spectrometric analysis of affinity-purified proteasomes. *Mol Biol Cell* 11: 3425–3439, 2000.
76. Walzthoeni T, Claassen M, Leitner A, Herzog F, Bohn S, Forster F, Beck M, and Aebersold R. False discovery rate

- estimation for cross-linked peptides identified by mass spectrometry. *Nat Methods* 9: 901–903, 2012.
77. Wang D, Zong C, Koag MC, Wang Y, Drews O, Fang C, Scruggs SB, and Ping P. Proteome dynamics and proteome function of cardiac 19S proteasomes. *Mol Cell Proteomics* 10: M110.006122, 2011.
 78. Wang X, Chen CF, Baker PR, Chen PL, Kaiser P, and Huang L. Mass spectrometric characterization of the affinity-purified human 26S proteasome complex. *Biochemistry* 46: 3553–3565, 2007.
 79. Wang X, Guerrero C, Kaiser P, and Huang L. Proteomics of proteasome complexes and ubiquitinated proteins. *Expert Rev Proteomics* 4: 649–665, 2007.
 80. Wang X and Huang L. Identifying dynamic interactors of protein complexes by quantitative mass spectrometry. *Mol Cell Proteomics* 7: 46–57, 2008.
 81. Wang X, Yen J, Kaiser P, and Huang L. Regulation of the 26S proteasome complex during oxidative stress. *Sci Signal* 3: ra88, 2010.
 82. Wells JA and McClendon CL. Reaching for high-hanging fruit in drug discovery at protein-protein interfaces. *Nature* 450: 1001–1009, 2007.
 83. Xu P, Duong DM, Seyfried NT, Cheng D, Xie Y, Robert J, Rush J, Hochstrasser M, Finley D, and Peng J. Quantitative proteomics reveals the function of unconventional ubiquitin chains in proteasomal degradation. *Cell* 137: 133–145, 2009.
 84. Yang B, Wu YJ, Zhu M, Fan SB, Lin J, Zhang K, Li S, Chi H, Li YX, Chen HF, Luo SK, Ding YH, Wang LH, Hao Z, Xiu LY, Chen S, Ye K, He SM, and Dong MQ. Identification of cross-linked peptides from complex samples. *Nat Methods* 9: 904–906, 2012.
 85. Zhang F, Hu Y, Huang P, Toleman CA, Paterson AJ, and Kudlow JE. Proteasome function is regulated by cyclic AMP-dependent protein kinase through phosphorylation of Rpt6. *J Biol Chem* 282: 22460–22471, 2007.
 86. Zong C, Gomes AV, Drews O, Li X, Young GW, Berhane B, Qiao X, French SW, Bardag-Gorce F, and Ping P. Regulation of murine cardiac 20S proteasomes: role of associating partners. *Circ Res* 99: 372–380, 2006.

Address correspondence to:

Dr. Lan Huang
 Department of Physiology and Biophysics
 University of California, Irvine
 Medical Science I, D233
 Irvine, CA 92697-4560

E-mail: lanhuang@uci.edu

Date of first submission to ARS Central, December 20, 2013;
 date of acceptance, January 14, 2014.

Abbreviations Used

2h	= yeast 2-hybrid system
CP	= core particle
cryoEM	= cryo-electron microscopy
DSSO	= disuccinimidyl sulfoxide
HB tag	= histidine-biotin tag
IVB	= <i>in vitro</i> binding assay
MS	= mass spectrometry
MS ⁿ	= multistage tandem mass spectrometry
PCI domain	= proteasome–CSN–eIF3 domain
PIP	= proteasome interacting protein
PPI	= protein–protein interaction
PTMs	= posttranslational modifications
QTAX	= quantitative analysis of tandem affinity purified <i>in vivo</i> cross-linked (x) protein complexes
RP	= regulatory particle
sc	= <i>Saccharomyces cerevisiae</i>
SILAC	= stable isotope labeling of amino acids in cell culture
sp	= <i>Schizosaccharomyces pombe</i>
TAP	= tandem affinity purification
Ub	= ubiquitin
UPS	= ubiquitin-proteasome system
XL-MS	= cross-linking mass spectrometry